energies

MDPI

Article

Steam Storage Rankine Cycle for Unutilized Applications in Distributed High-Temperature Waste Heat Recovery

Florian Raab [1,*], Lennart Böse [2], Harald Klein [3] and Frank Opferkuch [1]

[1] Technische Hochschule Nürnberg Georg Simon Ohm, Distributed Energy Conversion and Storage, Fürther Str. 246b, 90429 Nürnberg, Germany
[2] Professorship for Fluid Systems Technology, Friedrich-Alexander-Universität Erlangen-Nürnberg, Cauerstraße 4, 91058 Erlangen, Germany
[3] Institute of Plant and Process Technology, Technische Universität München, Boltzmannstraße 15, 85748 Garching, Germany
* Correspondence: florian.raab@th-nuernberg.de

Abstract: In the light of increasingly valuable resources and a trend towards more efficient processes pushed by climate change, distributed Waste Heat Recovery (WHR) is an important element in the transformation of the energy supply. In recent years, however, WHR systems have often been optimized and implemented for steady-state applications. In this paper, dynamic system modeling and a Steam Rankine Cycle (SRC) pilot plant with 40 kW_{el} are used to investigate applications unutilized thus far for the conversion of high-temperature waste heat into electricity using a shell boiler with 1.27 m^3 of liquid water for short-term energy storage. In addition to experimental investigations of the storage system as an Uninterruptible Power Supply (UPS) and the input and output of +/−100% electrical power peaks for grid-assistive operation, a control concept for the use of volatile waste heat is developed from a model-based controller design up to a Model Predictive Control (MPC) with the help of a dynamic system simulation. Based on the validated model and experimental measurement data, outlooks for concrete applications with higher storage capacity and power are provided.

Keywords: Steam Rankine Cycle; waste heat recovery; steam storage; experimental investigation; dynamic model

Citation: Raab, F.; Böse, L.; Klein, H.; Opferkuch, F. Steam Storage Rankine Cycle for Unutilized Applications in Distributed High-Temperature Waste Heat Recovery. *Energies* **2024**, *17*, 920. https://doi.org/10.3390/en17040920

Academic Editor: Flavio Caresana

Received: 9 January 2024
Revised: 6 February 2024
Accepted: 12 February 2024
Published: 16 February 2024

1. Introduction

Every energy conversion process is subject to losses, and the final energy form is mostly thermal energy. According to Forman et al. [1], 51.8% of primary energy was lost in waste heat in 2012, 20.6% of which with temperatures higher than 300 °C, 16.1% with temperatures between 100 and 300 °C, and 63.3% with temperatures <100 °C. Increasing financial pressure due to limited fossil resources, regulations on greenhouse gas emissions and marketing benefits are prompting global efforts to achieve higher efficiencies during energy conversion. If the Industrial Sector alone would convert the most valuable high-temperature waste heat (>300 °C) into electricity with an electrical efficiency of 15%, approx. 110 coal-fired power plants (of the existing 2215 worldwide [2]) with a mean net capacity of 525.2 MW_{el} could be replaced [2,3]. In a distributed energy supply, moreover, the energy of the heat sink can be used appropriately with the help of heat networks, creating maximally efficient processes.

Due to a variety of possibilities in the use of waste heat, operators are faced with the challenge of choosing the best solution for each application. In this decision-making process, the waste heat cascade is often used, which can be seen in Figure 1a. If waste heat cannot be avoided by optimizing the primary production process, it should first be used within the process. When the process does not require any further heat, internal use is recommended, e.g., for space heating or cooling. Should no heat be required in this area

either, the thermal energy can be converted to electrical energy. If this option also remains without advantage, external use via heat networks is suggested [4,5].

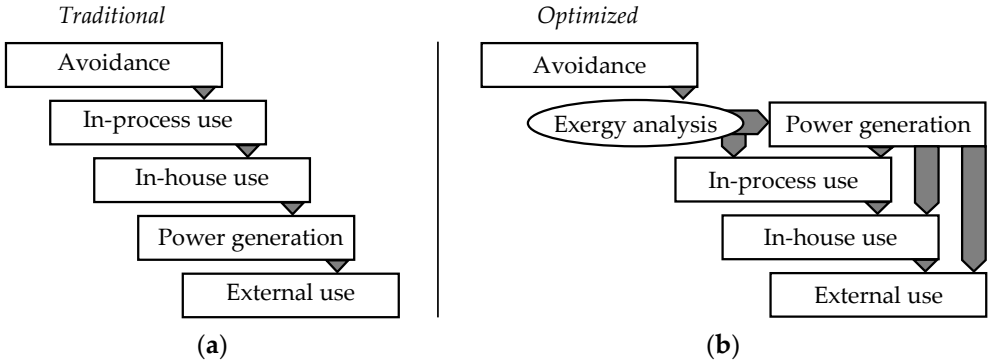

Figure 1. Traditional (**a**) and exergy-optimized (**b**) waste heat cascade for high-temperature Waste Heat Recovery.

The direct use of heat is realized via heat exchangers. In thermodynamic cycles, waste heat can either be used to provide heat at a higher or lower temperature level through sorption technology or converted into mechanical energy and thus electricity using power cycles. For power generation from waste heat, which is the focus of this work, different technologies have been established for varying temperatures and power levels of the source. For smaller power levels in the range of <1.000 kW_{el} and temperatures above 650 °C, Stirling engines can be applied [6]. In the range of less than 1 kW_{el} up to more than 10 MW_{el} and temperatures below 300 °C, the Organic Rankine Cycle (ORC) mainly provides efficiency advantages since the substance properties of the working medium can be adapted to the waste heat source using a variety of fluids. The Steam Rankine Cycle (SRC) is mainly used with large-scale power plant technology at temperatures above 300 °C [7]. For outputs below 10 MW_{el} and down to a few kW, the medium water poses challenges for the apparatus technology, which are currently being overcome in research projects [8]. In addition to the thermodynamic differences from the ORC, which become minimal from a waste heat temperature of about 400 °C, water as a working medium brings advantages in terms of sustainability and safety. Furthermore, direct energy storage in the circuit medium can be realized more safely [9].

Several technologies for Waste Heat Recovery (WHR), depending on the temperature and power of the waste heat, are therefore technically and economically available. In consequence, an exclusively one-dimensional examination of the use of waste heat, as in the waste heat cascade, is not always appropriate. In addition to the prevailing input temperature of the heat source, differences in the further possible steps of the process—internal, in-house and external use—must be taken into account. For this purpose, exergy, i.e., the energy that can be converted into any other form of energy, is not related to the environment but to the prevailing useful waste heat conditions in the next possible cascade. In a heat engine, thermal energy can then be converted into electrical energy with a thermal efficiency consisting of the Carnot efficiency and an exergetic efficiency [10]. A techno-economic analysis of waste heat and possible technologies for WHR must be added to this exergetic consideration in order to be able to make a decision in a respective application. The process of the proposed optimized waste heat cascade is shown in Figure 1b.

In particular, when chemical energy carriers such as natural gas or hydrogen are used to provide process steam or heat, which are cost-intensive due to taxes, transportation, the international energy market or energy-intensive production from renewable energy, the conversion of valuable exergy into electricity must be considered. The generated electricity then has significant efficiency and cost advantages compared to electricity supplied from the grid as a very high level of overall efficiency can be achieved through cogeneration.

The largest absolute Carnot potential, i.e., the highest proportion of exergy, is in waste heat from the transport sector. Mobile combustion engines, which are still the state of the art worldwide, emit more than 80% of primary energy into the environment as waste heat. Approaches to convert parts of these flows into electricity, e.g., the investigation in [11], have not been able to gain great acceptance in the automotive market and the commercial vehicle sector. The increasing use of e-mobility and hydrogen fuel cells will reduce this share in coming years.

However, industrial applications will still not be able to be fully electrified. Current efforts by energy-intensive companies, e.g., in the steel industry, see hydrogen as a key technology of the future. The challenge with recovering industrial high-temperature waste heat lies in the process conditions. Highly volatile temperatures and mass flow rates have often made WHR not possible or economical thus far. By designing according to the average waste heat power, much valuable energy will still be lost; however, by designing according to the maximum waste heat power, much cost-intensive plant capacity will remain unused most of the time. In the case of frequent outages of waste heat up to the standstill of the WHR, additional energy is lost in the partial load of the turbine, and the service life of the apparatus is shortened. A storage system allows the WHR system to be designed for the average power of the waste heat, buffers power peaks and overcomes outages.

To overcome these challenges, several options for converting volatile waste heat into electricity have already been investigated. Some approaches suggest adapting the exhaust gas or Rankine fluid mass flow rates in the case of volatile waste heat [12]. Popp et al. [13], on the other hand, investigate an adaptive turbine nozzle geometry in order to maintain the design pressure gradient across the turbine even with a partial load. Other approaches make use of thermal storage. According to [12], sensible storage systems like molten salt and intermediate oil circuits or latent storage such as steam accumulators and Phase-Change Materials (PCMs) are potential solutions for waste heat to power systems. Pili et al. [14] suggest different optimal economic solutions depending on the application. For the conversion of exhaust gases from the reheating furnace of a rolling mill into electricity, the configuration of a minimum waste heat flow and bypassing surplus exhaust gas, latent heat storage for the WHR of clinker-cooling air and a system without storage for an electric arc furnace are recommended. Bause et al. [15] installed a saturated-steam intermediate circuit as a buffer for volatile waste heat in combination with an ORC. Arabkoohsar [16], for example, considers a packed bed of stones, Nardin et al. [17] investigate PCM storage and Pantaleo et al. [18] analyze a sensible pressurized water cycle for storing thermal energy. Murakoshi et al. [19] integrate separate steam storage into a Steam Rankine Cycle. Schlüter et al. [20] examine an exhaust-gas-side regenerator unit for buffering waste heat from an aluminum die-casting furnace.

Adjusting the operating parameters in the Rankine cycle also leads to fluctuations in the turbine output analogous to the waste heat power. The thermal storage systems considered so far, on the other hand, shift the buffer function to an additional apparatus, which leads to high additional costs. The approach of the present work combines the advantages of both options and investigates thermal storage in the existing steam generator of a Rankine cycle with the parallel adjustment of the operating parameters over the turbine. The challenges of the design and transient operation of such plants are discussed below through simulative and experimental investigations. In addition to the buffer function of volatile waste heat and the resulting steady-state operation of the WHR system, other applications can be accessed through the storage system. Its use as an Uninterruptible Power Supply (UPS) for the absorption of renewable surplus electricity and for the release of power peaks will also be discussed.

2. Materials and Methods

In this section, the methodological approach of the present paper is described, including the experimental setup, the MicroRankine pilot plant and a dynamic system model using Modelica/Dymola.

2.1. MicroRankine Pilot Plant

The approaches investigated in the present work are experimentally based on the MicroRankine pilot plant at the Technische Hochschule Nürnberg Gerog Simon Ohm [8]. The plant, shown in Figure 2, was commissioned in 2020.

Figure 2. MicroRankine pilot plant at the sewage treatment plant in Nürnberg.

Since then, it has been converting electricity from the waste heat of a JMS 312 GS-B.L Internal Combustion Engine in continuous research operation. According to the data sheet, the waste heat has a temperature of 451 °C, and when cooled to 170 °C in the design case, transfers 247.6 kW_{th} to the working medium. The steam generator, which represents energy storage in this study, consists of a preheater, an evaporator and a superheater. The preheater is designed as a crossflow finned tube heat exchanger, with the exhaust gas flowing around the outside of the finned tubes and the water in the plain tubes being preheated to saturation temperature at an operating pressure of 16 bar. It has a weight of 500 kg, a filling capacity of 19.6 L of water and is made of P250GH. The evaporator is a shell boiler in which the exhaust gas flows through the plain tubes and the water evaporates in the shell space on the tubes. It is also made of P250GH and has a net weight of 2550 kg. Figure 3 shows the layout of the steam boiler. In a steady state at 50% filling level between the top of the tubes and the maximum filling level, there is 1.27 m^3 of water in the boiler.

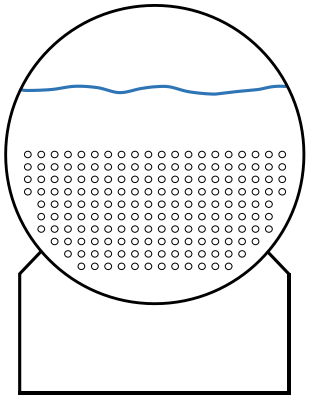

Figure 3. Layout of the steam boiler with exhaust gas tubes and water/steam chamber.

The superheater is made of 1.4571 and weighs 800 kg in when empty, with a filling volume of 69.7 L. It is designed as a crossflow shell-and-tube heat exchanger, with the steam being superheated inside the plain tubes and the exhaust gas flowing around the tubes. The steam is superheated up to 430 °C and then flows into the turbine, which expands the steam to vacuum with an isentropic efficiency of 53.2% under design conditions, with the generator feeding up to 40 kW_{el} into the grid. The water-cooled asymmetric plate condenser

with dimples forces the steam to condensate at an absolute pressure of 0.06–0.2 bar. The condensate flows into the hotwell and is finally pumped by a piston membrane pump back into the preheater, where the process starts from the beginning. The experimental setup was described in detail in previous work by the authors [8].

In contrast to most steam generators in distributed ORC systems, the evaporator here was designed as a shell boiler. This type of construction is the industrial standard for waste heat steam boilers as it allows for relatively simple control via the filling level, and impurities always remain in the steam boiler. However, due to pool boiling and the lower heat transfer coefficient compared to flow boiling in a forced-flow apparatus, such a shell boiler is less compact and has a higher capital expenditure as a result of more material consumption. In addition, the resulting higher volume of pressurized liquid–gas mixture in the interior poses an increased hazard. According to Directive 2014/68/EU [21], this circumstance has an influence on safety equipment, approval and operation and thus increases both capital expenditure and operational expenditure.

The steam boiler in the experimental setup, with a filling level of liquid saturated water and saturated steam in the space above, in combination with the regulation valve before the turbine, represents energy storage comparable to Ruth's storage tanks, which have been in use since the beginning of the 20th century [22]. Due to an additional pressure drop through the partially closed control valve, the pressure in the boiler can be increased, and thermal energy can be stored. When the valve is opened and the pressure decreases, the saturated liquid evaporates, and a higher steam mass flow rate is discharged immediately over the surface of the liquid phase. In addition to the latent heat of the water/steam mixture, the tubes and the boiler shell also store sensible heat, which leads to evaporation at their surfaces when the pressure drops. The storage capacity of the superheater, largely due to the stainless steel mass, ensures that superheating is maintained for some time even if heating fails. The combination of evaporation and storage in one apparatus instead of in two separate apparatuses has benefits in terms of cost. Due to the safety equipment for the steam boiler used in the MicroRankine plant, a storage pressure of more than 17.5 bar was not possible as the plant's technology was originally designed for a steady state.

In addition to the use of high-temperature PCMs in steam boilers [23], an increase in storage capacity can be achieved primarily through higher storage volumes and storage pressures. These options will be considered in the following investigations when expanding the areas of application.

2.2. Dynamic Model of the System

To design a process and the key components, studies must be carried out under transient operating conditions. Acausal, object-oriented and multiphysical simulation methods such as DYMOLA are particularly suitable for mapping the behavior of the components and the balance of plant in order to be able to carry out simulation studies efficiently.

The dynamic model of the system, whose graphical interface can be seen in Figure 4, was based on the modeling language Modelica using the program Dymola and the detailed model libraries TIL and TILMedia [24] as a basis. This object-oriented approach allows for complex systems of differential algebraic equations (DAEs) to be solved in an exchangeable and reusable way. The main apparatuses of the MicroRankine SRC, the pump, steam generator, turbine and condenser, were modeled and compared with measured data in the steady state and during transient operations. The individual devices are described in more detail below.

The piston membrane pump was evaluated with variable piston strokes at different stroke frequencies, and a black-box characteristic map for the mass flow rate and electrical power and efficiency was developed. While white-box models are derived from physical models, black-box models are characterized by mathematical models that are created by evaluating experimentally determined input and output variables. Due to the operating principle of the metering pump, the mass flow rate is hardly pressure-dependent, and

pressure-stiff characteristic curves of the flow rate, electrical power and efficiency result which are linearly dependent on stroke length and stroke frequency.

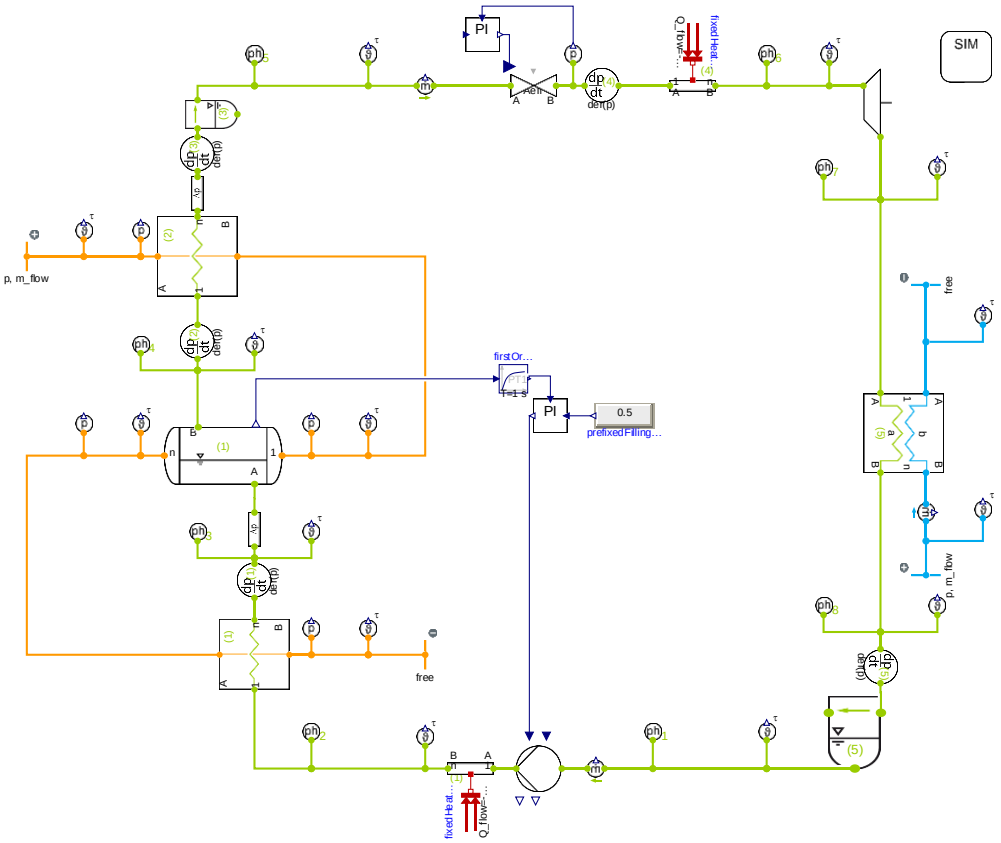

Figure 4. Graphical interface of the Modelica simulation model in Dymola.

The preheater with finned tubes was described using a 1D model that calculated the heat transfer and heat conduction processes on the insides of smooth tubes, inside the tube walls and on finned tube bundles according to the current literature for the different materials. In the steam boiler, the heat transfer coefficient from the exhaust gas to the inside of the tube, the heat conduction inside the tube and the heat transfer coefficient during evaporation on the outside of the tube bundle are also described by correlations from the literature. In addition, the resulting volume that the vapor bubbles occupy when rising in the liquid phase was calculated, and in combination with the physical properties of the water under operating conditions, a filling level was calculated which was controlled by the pump using a PI controller in the model. The superheater was calculated using correlations from the literature for single-phase heat transfer in a crossflow heat exchanger with a smooth tube bundle.

The valve upstream of the turbine, which will be the application case for control design in the future, was based on calculations according to DIN 60534-2-1 [25] and DIN 60534-2-3 [26] using manufacturer data. In the turbine model, the isentropic turbine efficiency was calculated as a function of the pressure ratio with the help of geometric variables of the turbine such as flow angles, nozzle efficiency and diameter. The condenser heat transfer coefficients were approximated using a library model for plate heat exchangers with a herringbone pattern, using the plate area and the number of plates of the installed device. The hotwell represents an ideal separator with a given internal volume.

With the help of steady-state measurement data from the MicroRankine pilot plant, the steady-state results of the system simulation were fitted. Parameter studies were used to determine linear correction factors for the heat transfer coefficients in the preheater, steam boiler, superheater and condenser, the fin efficiency in the preheater, the pressure losses

over the apparatuses, the electrical efficiencies in the regenerative unit and the geometric parameters in the condenser. Heat losses were estimated and also fitted with the measured data in combination with the heat transfer coefficients.

For the dynamic fitting of the model, measurement data during a generated failure of the heating in the experimental setup were reproduced in the simulation model with the same process conditions. The masses of the tubes were already included in the DAE system through the calculation of thermal conduction. The masses of the housings and the attachments of the apparatuses were estimated using their documentation and added to the heat exchanger models with a resistance–capacitance model. In the next step, the process conditions on the water/steam side after 20 min without heating were used as a target value, and the model was fitted by varying the additional mass and its corresponding heat transfer coefficients to the fluid.

In order to check the consistency of the model with other transient processes, a volatile waste heat flow was realized in the MicroRankine plant by opening and closing the exhaust gas flap with a superimposed sinusoidal oscillation. The result was fluctuating steam boiler pressure. Figure 5 shows this fluctuating boiler pressure, measured with the experimental setup and the result of the steady state and transient fitted simulation model with the same input parameters for the exhaust gas.

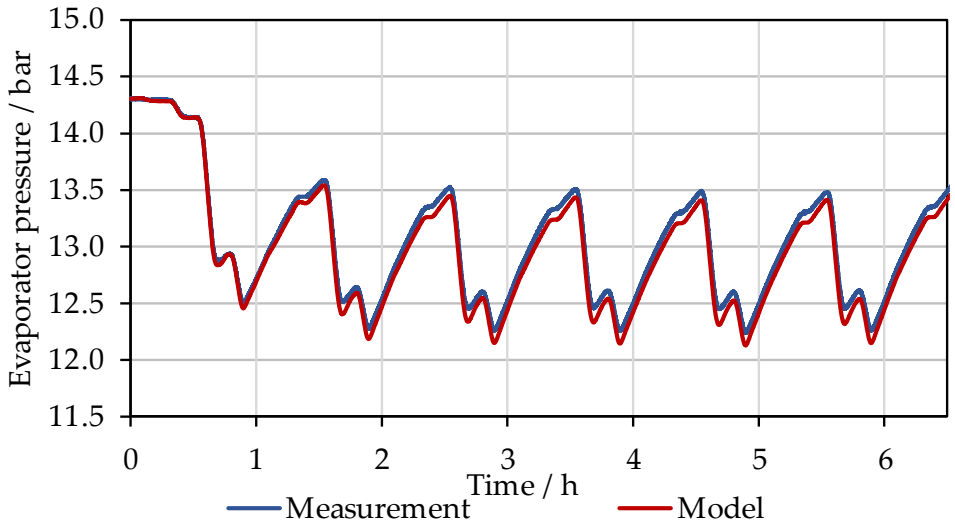

Figure 5. Fluctuating pressure in the steam boiler due to volatile exhaust gas mass flow rate—measurement with the experimental setup and the result of the fitted simulation model.

After the steady-state conditions, in which the model matches the measurements very well, very good agreement can also be seen in the first range of pressure reduction as the transient fitting of the model was performed with a similar process. In the stable fluctuating state, a difference between the curves can be seen, but the simulation reproduces reality sufficiently accurately for further investigations. A more precise adjustment would be possible with further measurements and a more extensive fitting but is not relevant for the following applications.

The prerequisite for the following investigation is, therefore, a highly automated industrial SRC experimental setup with a steam generator combined with a steam accumulator and a sufficient fitted dynamic simulation model.

3. Results and Discussion

After the background of the present research work as well as the model-based and experimental fundamentals have been explained, the following section will discuss specific applications that can be demonstrated with the help of the experimental setup and the simulation. For each application, an outlook of area-wide use or possible necessary scaling

is discussed. First, the application of the system as a UPS is presented, supported by various measurement series and scaling of the storage. Then, the conversion of volatile waste heat into electricity by buffering in the steam boiler with the development of a model-based controller design up to a Model Predictive Control (MPC) is presented. This is supported by an application to a real waste heat profile. Finally, the system's application and extension to grid-assistive operation are discussed.

3.1. Uninterruptible Power Supply

A UPS is a device that supplies power in the event of grid failure. These can be safety-relevant facilities, e.g., for the emergency cooling of processes or the magnetic bearings of high-speed machines, but they can also be system-relevant facilities such as water supply facilities, sewage treatment plants or health facilities. The higher the negative effects of a power failure, the higher the demands on the UPS. According to DIN EN IEC 62040-3 [27], a distinction is made between three classes of UPSs. In Class 3, the switching time is 4–10 ms, the switching time is 2–4 ms in Class 2 and a continuous sinusoidal voltage is generated in Class 1. The rapid start times in many cases only bridge short periods until emergency power generators that have longer start-up phases come into operation. There are technical solutions for all three classes wherein battery storage is most commonly used.

The intelligent use of existing resources with already available steam generation in combination with a steam turbine, e.g., in hospitals or the food industry, could replace a Class 1 battery UPS or supplement it for further safety. The energy stored in the steam can be sufficient to fill time until emergency power-capable combustion engines start up. The steam stored in the steam boiler, in combination with the turbine, generates electricity for a certain time in the event of the failure of all heating whereby the pressure and turbine output decrease over time. In the following section, the storage capacity of the steam boiler of the MicroRankine pilot plant is investigated experimentally under different process conditions. Then, extensions to its storage capability are simulated using the system model.

3.1.1. Experimental Investigation of the System in the Case of Heating Failure

During steady-state operation, a filling level between 30 and 70% can be set between the upper end of the boiler tubes and the maximum filling level. Figures 6 and 7 show with full lines the pressure in the steam boiler and the electrical power supplied to the grid with the heating is switched off for initial filling levels of 30, 50 and 70% after five minutes.

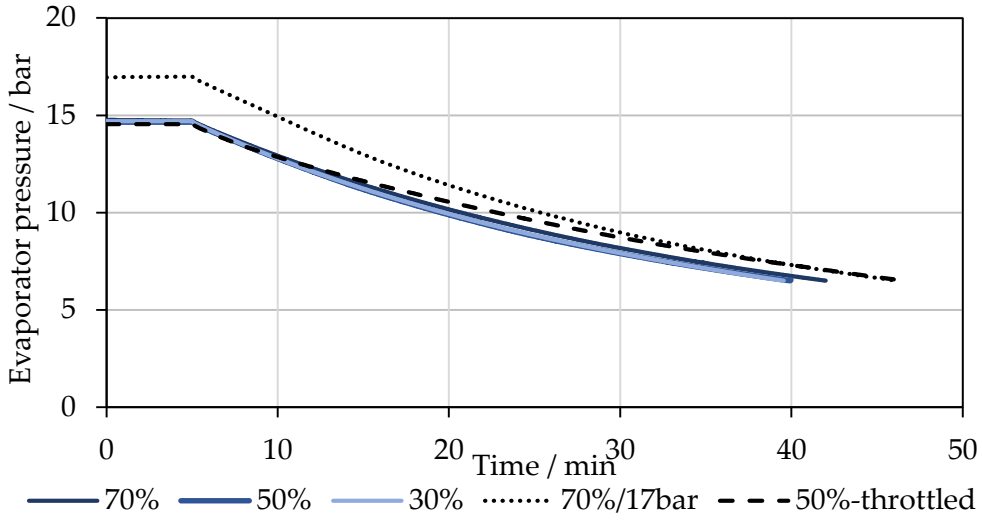

Figure 6. Evaporator pressure during shutdown with different start conditions.

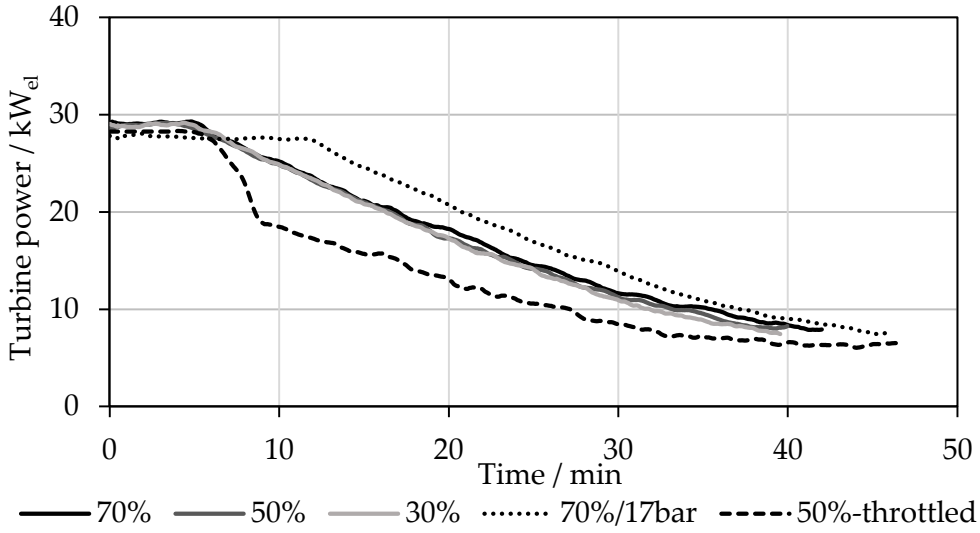

Figure 7. Turbine power during shutdown with different start conditions.

Table 1 shows the average turbine output after the heating failure, the total stored electrical energy, the time between switching off the heating and 6.5 bar steam boiler pressure and the level of superheating at the end. When the pressure fell below 6.5 bar, the turbine was switched off to prevent drop erosion. A turbine that can expand from lower pressures could also feed in power beyond this point.

Table 1. Summary of the measured storage capacity with different start conditions.

Start Conditions		**70%—17 bar**	**70%**	**60%**	**50%**	**40%**	**30%**	**50%—Throttled**
Mean turbine power	[kW$_{el}$]	17.6	16.6	16.2	16.6	16.2	16.5	11.9
Total el. energy	[kWh$_{el}$]	12.1	10.2	10.0	9.7	9.5	9.5	9.3
Time	[min]	46.2	42.0	41.9	40.0	40.3	39.6	46.6
End superheating	[K]	145.8	157.9	158.2	163.0	164.6	166.1	164.0

Different initial states only bring small changes in this case. Between 30 and 70% filling levels, there is approx. 304 L more liquid water in the boiler, and 0.7 kWh more electrical energy can be stored for an additional 2.4 min.

In the next test, an additional pressure drop was created by the valve in front of the turbine, which increased the pressure in the boiler to approx. 17 bar (dotted lines). After the heating fails, the pressure after the valve is controlled to a constant value, which means that the turbine continues to feed power into the grid at a nearly constant level for a few minutes before decreasing, and the pressure in the boiler slowly decreases from the beginning. In total, with a start level of 70% and 17 bar, 2.4 kWh$_{el}$ more could be stored compared to the regular state at 50% and for 6.2 min longer, power could be fed into the grid.

In the event of a heating failure, steam withdrawal can also be delayed by throttling the valve in front of the turbine from the beginning of the failure. The dashed lines show this as an example wherein over a period of an additional 6.6 min compared to the 50% start conditions, power is fed to the grid but, is overall 0.4 kWh$_{el}$ less due to the additional pressure loss. During steady-state operation, the steam at the outlet of the superheater is superheated by approx. 220 K to prevent drop erosion in the turbine. In all the tests described here, superheating of at least 146 K was still available at the end, despite the heating failure.

3.1.2. Simulation-Based Expansion of Storage Capability

In order to investigate a possible variation in the storage capacity of the steam boiler, the shutdown of the plant was simulated next to the original system (black line) with +2000 L storage volume (dashed line), with +15 bar storage pressure (dotted line) and a combination of these two (+2000 L/+15 bar—dashed–dotted line). In Figure 8, the evaporator pressure, the turbine inlet pressure and the turbine power are displayed.

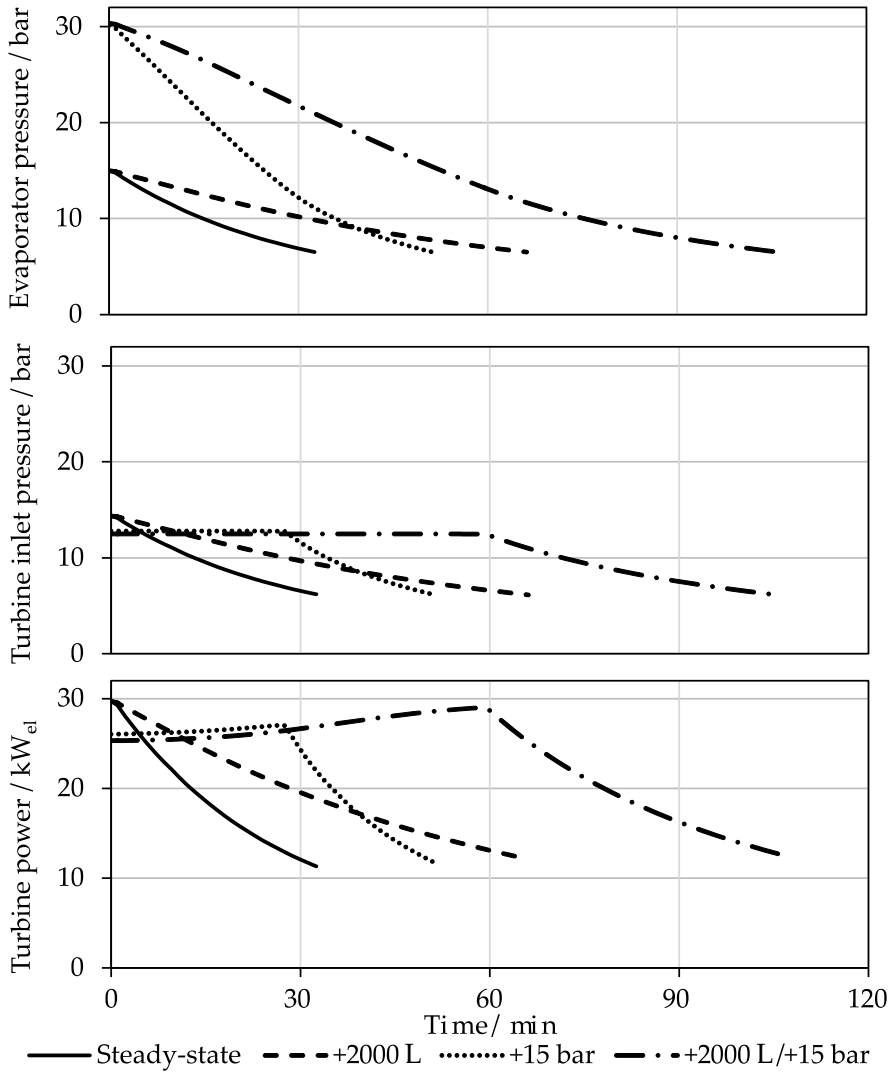

Figure 8. Simulated evaporator pressure, turbine inlet pressure and turbine power during shutdown according to a simulation of the original MicroRankine setup, with +2000 L liquid storage volume, +15 bar storage pressure and combined +2000 L/15 bar start conditions.

The two individual variations each yield an increase in storage of +104% (+2000 L) and +58% (+15 bar) in time and +91% and +68% in electrical energy supplied, respectively, while the combination yields a factor of 3.3 in time and 3.5 in energy. However, the superheating of the live steam is reduced to 28 K in the last case, according to the model.

3.2. Volatile Waste Heat

Volatile waste heat challenges a WHR system without storage as plants either cannot use a large part of the energy due to undersizing or cannot be operated economically due to oversizing. A highly transient operation of a plant is also disadvantageous for the operating life of its apparatuses. Furthermore, if the waste heat power fails and electricity generation is thus interrupted, the grid consumption increases, which can generate cost-intensive

peak loads. The following study is intended to investigate the use of the steam boiler as a storage unit to compensate for fluctuations in waste heat. For this purpose, a volatile waste heat profile was imposed on the MicroRankine plant via the exhaust gas flap. The input parameters of the waste heat mass flow rate and the temperature can be seen in Figure 9. The waste heat decreases by approx. 67.6% over several minutes at an almost constant temperature. On average, the waste heat corresponds to 201 kW_{th}.

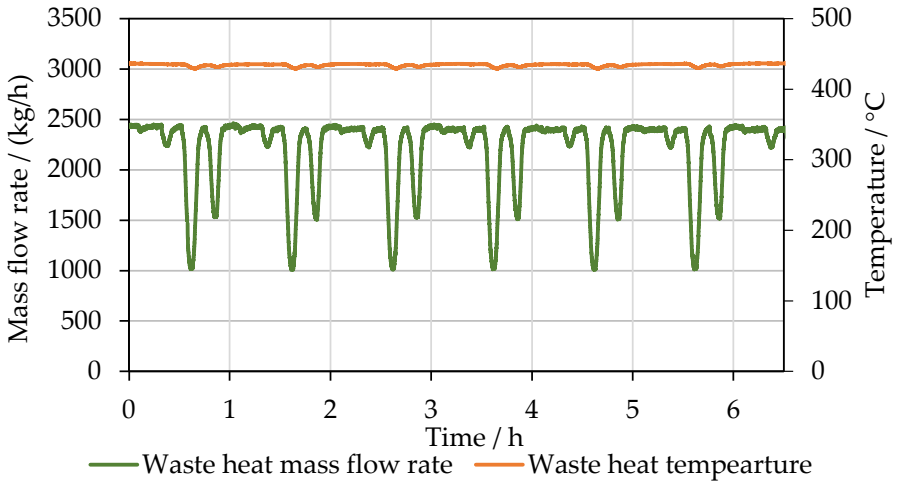

Figure 9. Volatile waste heat mass flow rate and temperature through exhaust gas flap control.

Without further control, the fluctuation in waste heat power is already partially damped in the WHR system. Figure 10 shows the pressure in the steam boiler and the power that the turbine feeds into the grid, both rising and falling with the waste heat. The turbine output fluctuates by only 11.7% more than during steady-state operation.

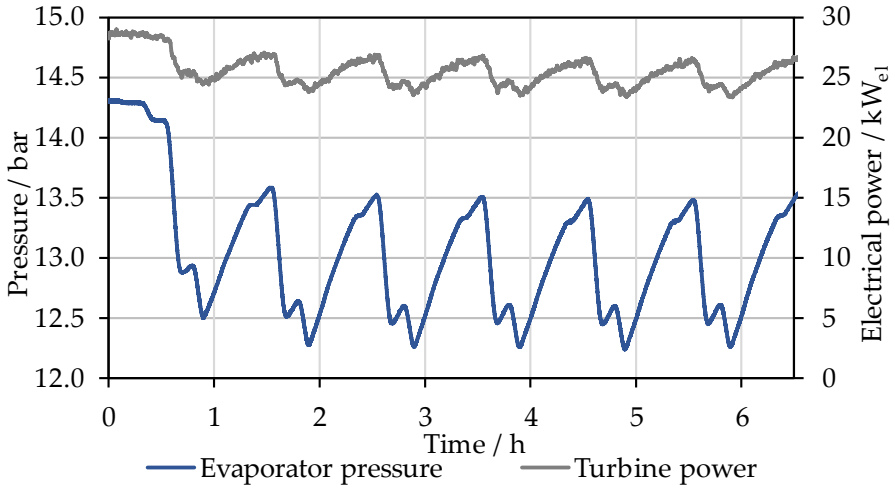

Figure 10. Turbine power and evaporator pressure during volatile waste heat.

To compensate for the remaining fluctuations, the valve upstream of the turbine has to be controlled so that the pressure downstream of the valve, i.e., in the turbine inlet, remains constant. A constant pressure ratio across the turbine leads to a constant output. The pressure in the steam boiler continues to fluctuate but at a higher level. To further compare the quality of the control, the standard deviation of the turbine inlet pressure is considered. In steady-state operation, this is 0.0061; in volatile operation without control, it is 0.38.

In designing the pressure to be controlled, the model is already helpful. If the control variable is selected too high, the pressure in the accumulator will partly drop below the

control variable, and the turbine output will decrease with 100% valve position. If the control variable is selected too low, the pressure in the steam boiler increases unnecessarily, which leads to further losses due to expansion in the valve and the safety limits being exceeded.

In the following subchapters, the design of this controller and the use of the dynamic model are examined. First, a static PI controller is designed with the help of the model using common methods, followed by a dynamic PI controller with gain scheduling. Subsequently, the model itself is used to realize a Model-Based Control (MBC) system with and without closed-loop control. Finally, it is demonstrated how Model Predictive Control can be implemented, and the advantages of these control systems are discussed.

3.2.1. Model-Based Controller Design: Static PI Controller

The Ziegler–Nichols method of turning tangents is first used to determine appropriate parameters for the gain and reset time of a PI controller in a closed loop, as seen in Figure 11. For this purpose, a step signal is applied to the valve position in the system model and the step response of the pressure downstream of the valve is evaluated, from which the gain and reset time result.

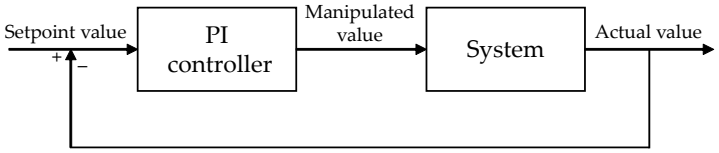

Figure 11. Closed control loop applied to the valve upstream of turbine with PI controller.

The result of the implemented controller can be seen in Figure 12, where the pressure values before and after the valve are shown.

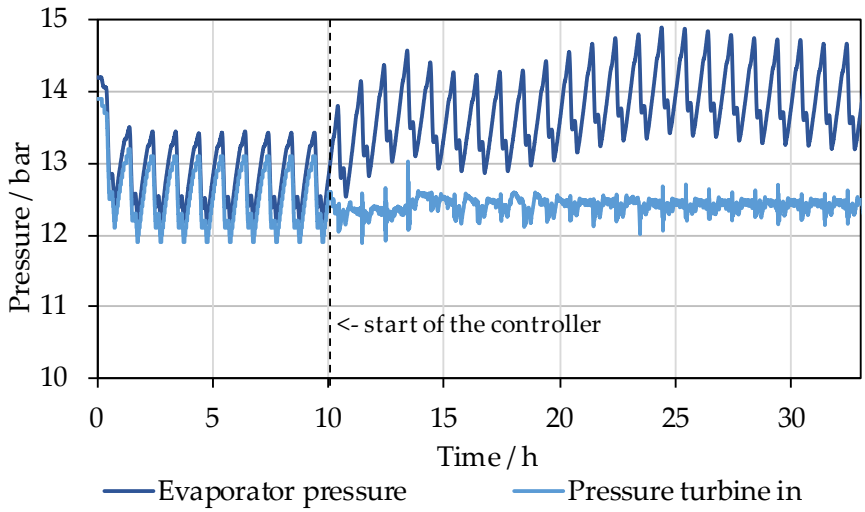

Figure 12. Evaporator and turbine inlet pressure during volatile waste heat flow and with PI controller.

From hour 10, the controller is activated, and the system is regulated to a constant pressure upstream of the turbine. In a steady state, a strong oscillation of the controlled variable can still be seen. As a result, the turbine power still fluctuates by +1.0% more than in the steady state, and the standard deviation of the turbine inlet pressure is 0.058. The reason for the fluctuation is the static controller in a non-linear control task. For this reason, a dynamic PI controller will be developed in the next step.

3.2.2. Model-Based Controller Design: Dynamic PI Controller via Gain Scheduling

The design of the controller using the model was performed again for a dynamic controller at different starting valve positions and representative steps. The resulting gain and the reset time were determined in each case. Variable parameters result over the range of the valve position, which were integrated into the controller with the aid of a gain scheduler, as shown in the closed loop in Figure 13.

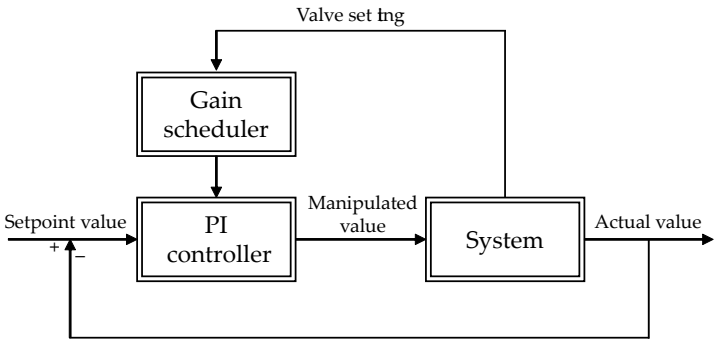

Figure 13. Closed control loop applied to the valve upstream the turbine with PI controller and gain scheduling.

The result can be seen in Figure 14, where, again, the pressure before and after the valve and additionally the valve position are displayed. The turbine power varies by +0.1% compared to steady-state operation, and the standard deviation of the controlled variable is 0.041.

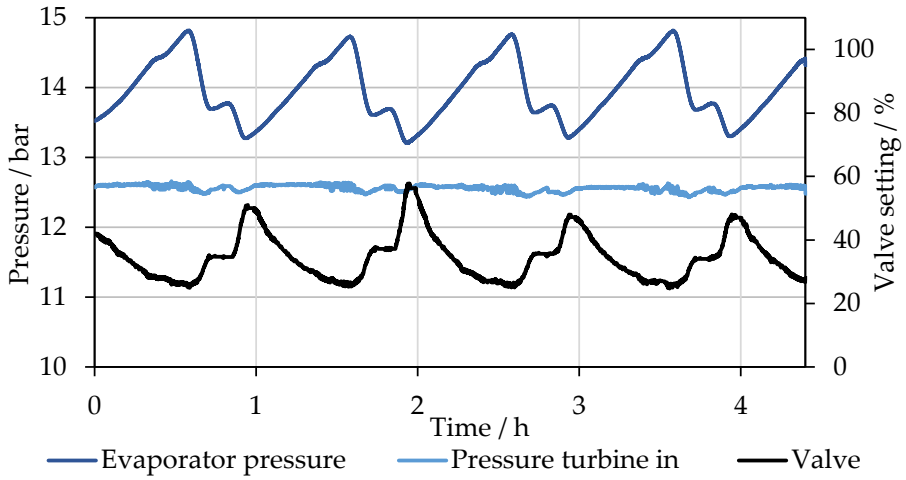

Figure 14. Evaporator and turbine inlet pressure, valve setting during volatile waste heat flow and PI controller with gain scheduling.

A significant improvement in control quality can be seen. To investigate whether further improvements can be achieved from the model, the model will be used in the next step to control the valve directly.

3.2.3. Model-Based Control

For MBC, a section of the entire system model was used, and an interface between the control and the simulation was implemented on a Python basis. The interface reads the measured data of the inlet pressure of the valve from the Programmable Logic Controller (PLC), simulates the optimal valve position to achieve the desired controlled variable and writes this valve position back to the PLC. This open loop is schematically shown in Figure 15.

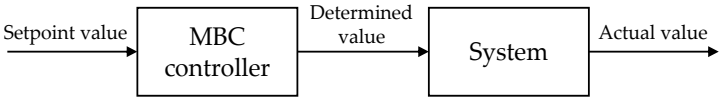

Figure 15. Open MBC loop applied to the valve upstream of the turbine.

In Figure 16, the PI controller was switched to MBC starting at hour 1.8. As can be seen, the valve position no longer oscillates since the controller does not attempt to compensate for the fluctuations that occur due to the dead band of the valve actuator. At the same time, it can be seen that the controlled variable deviates significantly from the setpoint in some areas.

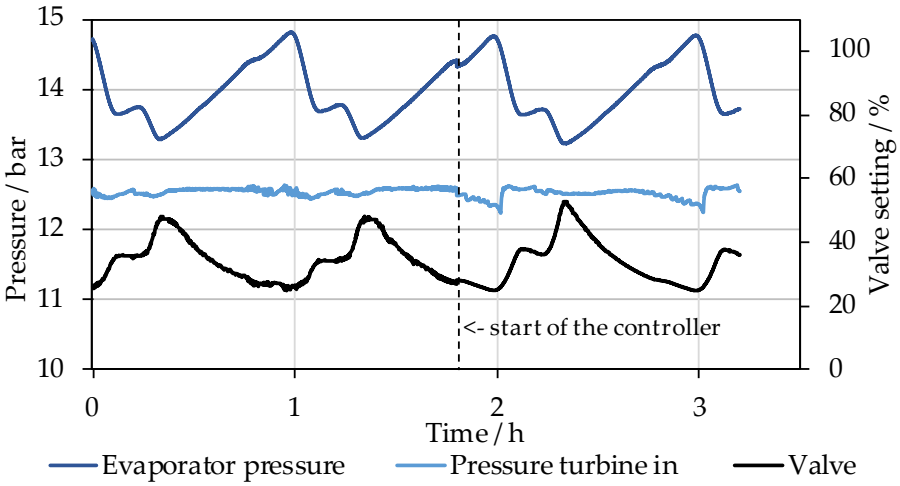

Figure 16. Evaporator and turbine inlet pressure, valve setting during volatile waste heat flow and open MBC loop.

The turbine output is almost equal to the control via the gain scheduler and the PI controller, but the standard deviation increases to 0.067. Thus, no improvement in control was created. The reason for this seems to be the valve model, which does not represent the physical processes sufficiently accurately in every area. Therefore, in the next step, the control loop was closed again, and the model was live-fitted with a linear fitting parameter, which is shown schematically in Figure 17.

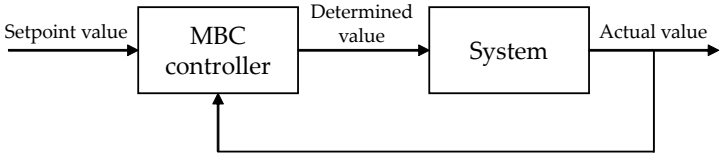

Figure 17. Closed MBC loop applied to the valve upstream of the turbine.

Figure 18 shows the result of this control. From hour 2.8, the controller was switched from PI to closed-loop MBC. Due to feedback, the valve position fluctuated slightly more than in the open approach. A fluctuation can still be seen in the controlled variable, but the standard deviation of the turbine inlet pressure was reduced to 0.035, creating a slight improvement.

Since the dynamics of the steam boiler were not taken into account in the previous controllers, a simple example is given below to show how predictive control can be implemented with the aid of the system model.

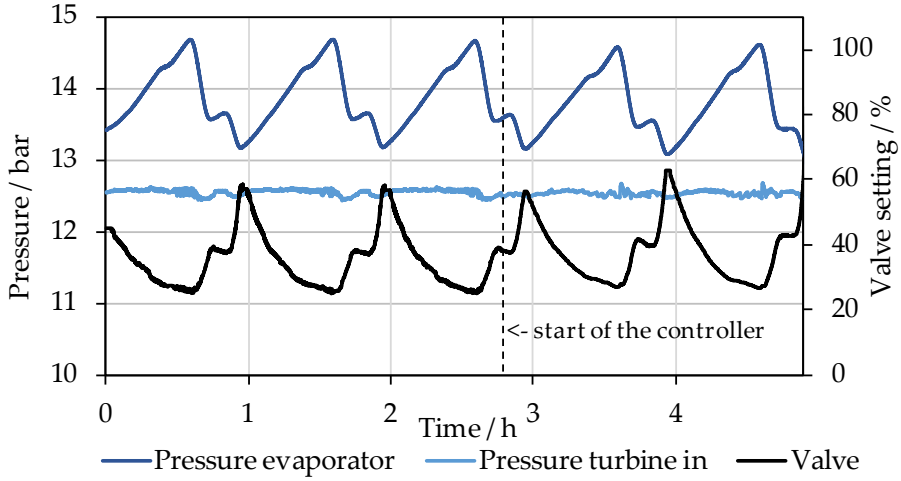

Figure 18. Evaporator and turbine inlet pressure, valve setting during volatile waste heat flow and with closed-loop MBC.

3.2.4. Model Predictive Control

MPC simulates using actual measured values faster than in real time, with the result being determined in advance. It was implemented in the MicroRankine system using the dynamic model and the interface as described. The controller system shown in Figure 19 detects a disturbance and transfers the measured values to the MPC controller, which determines a corrected variable which, in turn, can be transferred to the system.

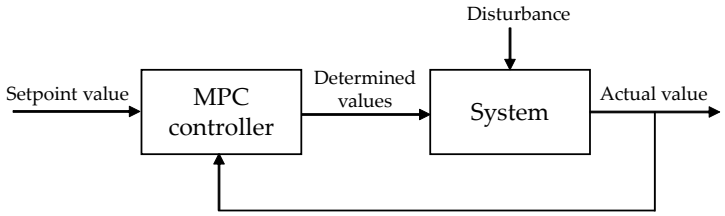

Figure 19. Closed MPC loop applied to the valve upstream of the turbine.

To illustrate this, at 0.8 h, a step change was applied to the exhaust gas while the turbine valve controlled a constant pressure. Figure 20 shows this step change in the mass flow rate of the exhaust gas, and for comparison, it also shows the response of the system with the previous PI controller. In more than 4.5 h, steady-state operation returns.

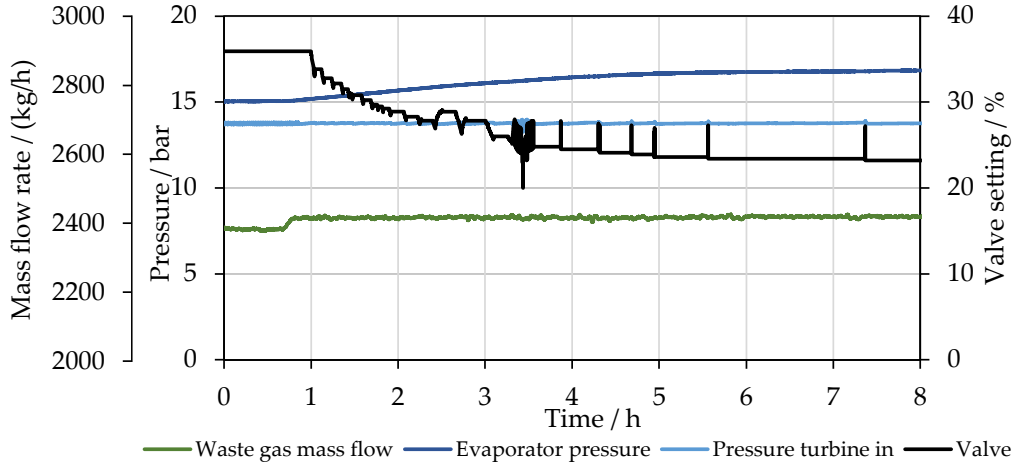

Figure 20. Exhaust jump, evaporator/turbine inlet pressure and valve setting with active PI controller.

The MPC as implemented in the MicroRankine pilot plant is shown in Figure 21. The controller detects the exhaust gas step and simulates the system using the PI controller. The resulting valve position, as soon as the system is in a steady state again, is transferred to the PLC. As can be seen, steady-state operation can be achieved after only about 2 h.

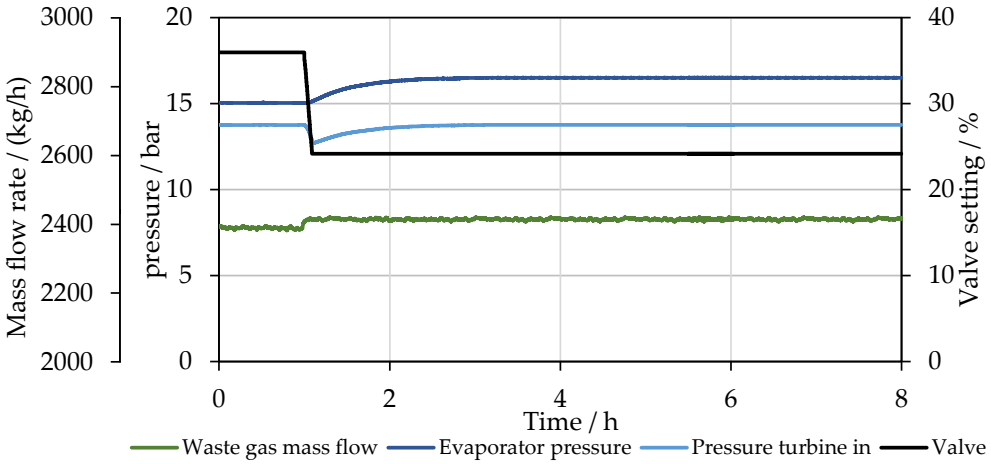

Figure 21. Exhaust gas jump, evaporator and turbine inlet pressure and valve setting with active MPC.

3.2.5. Application to a Real Industrial Waste Heat Profile

After investigating the conversion of volatile waste heat into electricity using the MicroRankine plant, the approach is applied to a real use case in the following subsection. Figure 22 shows the waste heat from two crucible furnaces from the casting industry, each with a firing capacity of 300 kW, as described in [28]. The actual exhaust gas temperature at the outlet of the furnaces is 1500 °C, which is reduced to approx. 400–450 °C by drawing in secondary air. The average waste heat output when cooled to 170 °C is 334.9 kW_{th}.

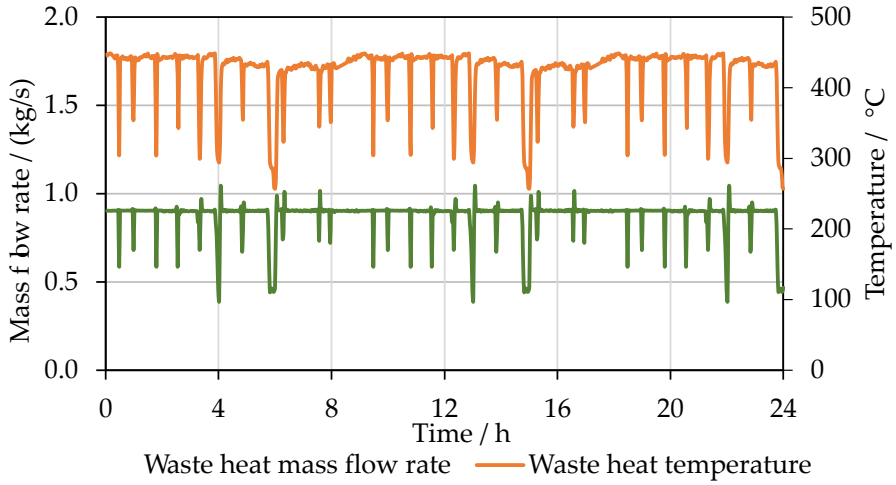

Figure 22. Waste heat mass flow rates and temperatures of two crucible furnaces from the casting industry, each with a firing capacity of 300 kW, according to [28].

If waste heat conversion is simulated using the MicroRankine pilot plant without further control, fluctuating pressure in the boiler and turbine inlet occurs, as shown in Figure 23, resulting in a fluctuating turbine output.

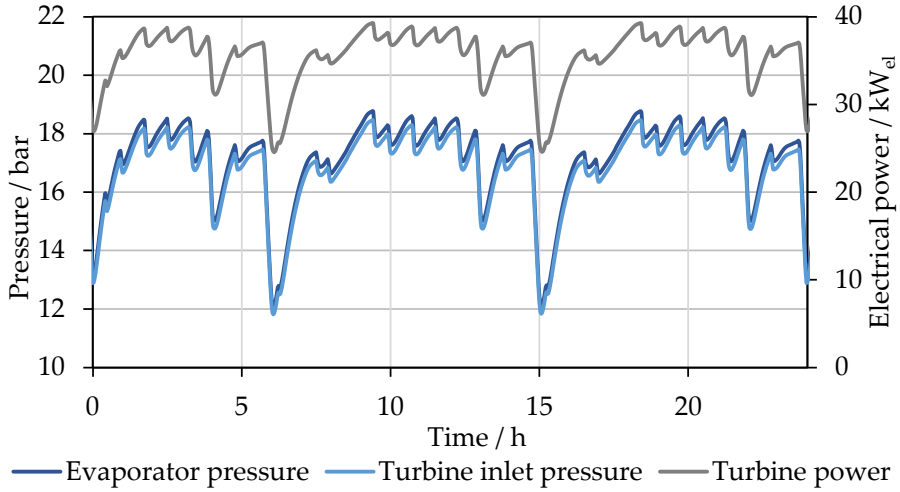

Figure 23. Simulated evaporator pressure, turbine inlet pressure and turbine power during volatile WHR for the crucible furnaces without control in the MicroRankine plant.

If the turbine inlet pressure is controlled to 15.7 bar, the fluctuation in turbine output is largely eliminated. A varying mass flow rate due to a moving pinch point and the varying superheating that occurs in each case lead to slight changes in the turbine output despite a constant pressure ratio. The simulation results can be seen in Figure 24.

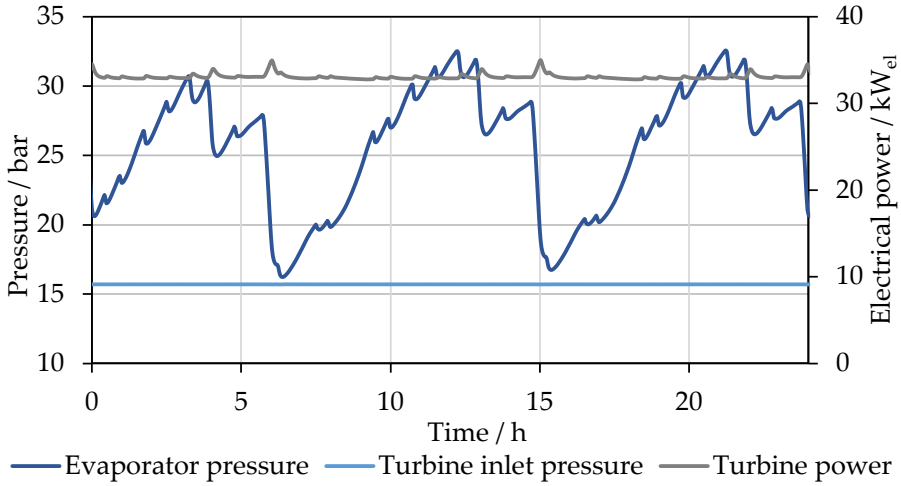

Figure 24. Simulated evaporator pressure, turbine inlet pressure and turbine power during volatile WHR for the crucible furnaces with a controlled valve in the MicroRankine plant.

3.3. Grid-Assistive Operation

Another application that can be accessed with the help of Steam Storage Rankine Cycles is grid-assistive operation. Here, a distinction can be made between industrial consumers and grid operators. Both suffer from peak loads. Due to an increase in renewable energies and weather-dependent fluctuations in the provision of power, distribution networks are increasingly reaching their limits, which leads to faster aging of the existing cables [29]. Since grid extension is associated with high costs, operators are trying to avoid overloads by means of intelligent controls and extensive planning. The so-called Redispath 2.0 in Germany [30], for example, partially shuts down systems feeding into the grid in the event of overload. In order to compensate for fluctuations in the transmission grid, control power at the European level is divided into Frequency Containment Reserve (FCR), automatic Frequency Restoration Reserve and manual Frequency Restoration Reserve, each of which must be able to receive or provide at least 1 MW_{el} after 30 s, 5 and 12.5 min. For an

FCR, a total ±3000 MW must be available in the European Network of Transmission System Operators for Electricity, and tendering for compensation takes place every four hours. So far, these services are mainly provided by pumped storage power plants but also battery storage, gas and coal-fired power plants [31].

Due to the increasing utilization of renewable energies, the demand for flexible loads will increase in the future. For industrial customers, this circumstance leads to high costs for unplanned peaks in purchased electricity. In Germany, for example, the user's electricity price for an annual consumption of more than 100,000 kWh is based on registering power metering according to a power price and an energy price, whereby in the power price, the peak loads are paid, which can account for the larger part of the total cost [32].

Distributed Steam Storage Rankine Cycle plants can help cover peak loads in these cases by storing and releasing steam abruptly via the turbine when needed, resulting in increased electrical output. When using Power-2-Heat with the help of electric heaters, regenerative surplus electricity can be stored in the system, which also leads to an increase in storage pressure. Compared to Murakoshi [18], the steam in the present approach can be stored directly in the steam boiler without an additional apparatus required. Figure 25 shows the simplified process flow diagram of this Power-2-Heat-2-Power system.

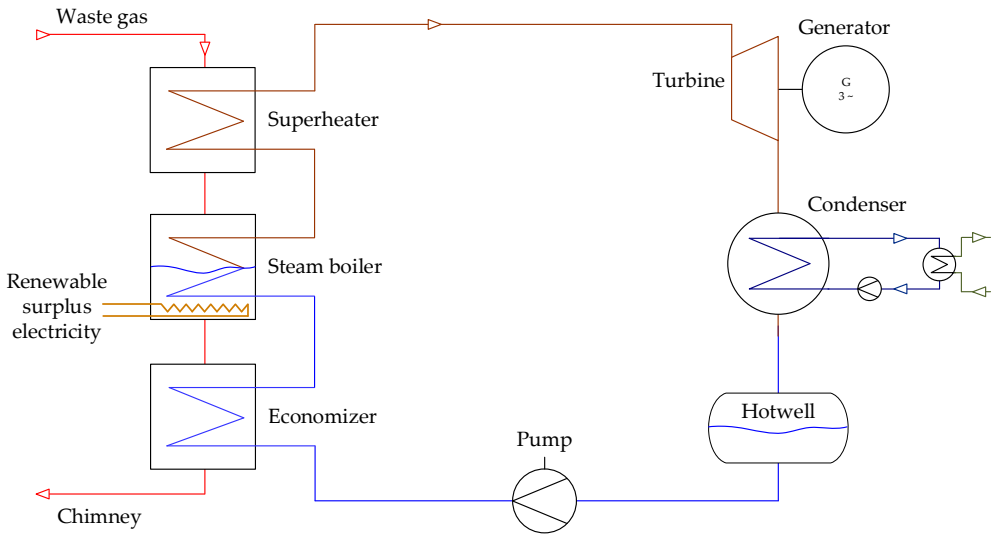

Figure 25. Schematic flow diagram of the SRC with Power-2-Heat for the integration of renewable surplus power.

Thus, the plant technology can absorb or release power peaks at nodes in the distribution grid, participate as an FCR in the transmission grid for plants smaller than 1 MW_{el} through so-called pooling or cover peak loads for industrial customers. The possibilities of this type of peak shaving are evaluated experimentally and model-based on the following.

3.3.1. Experimental Investigation of Power Peaks at the MicroRankine Pilot Plant

Figure 26 shows the storage process in the steam boiler of the MicroRankine pilot plant from steady-state operation to approx. 17 bar storage pressure with the boiler pressure, the turbine inlet pressure and the valve setting. In order to influence the turbine output minimally, the valve upstream of the turbine was only slowly throttled, resulting in a storage process to a steady state taking approx. 8 h.

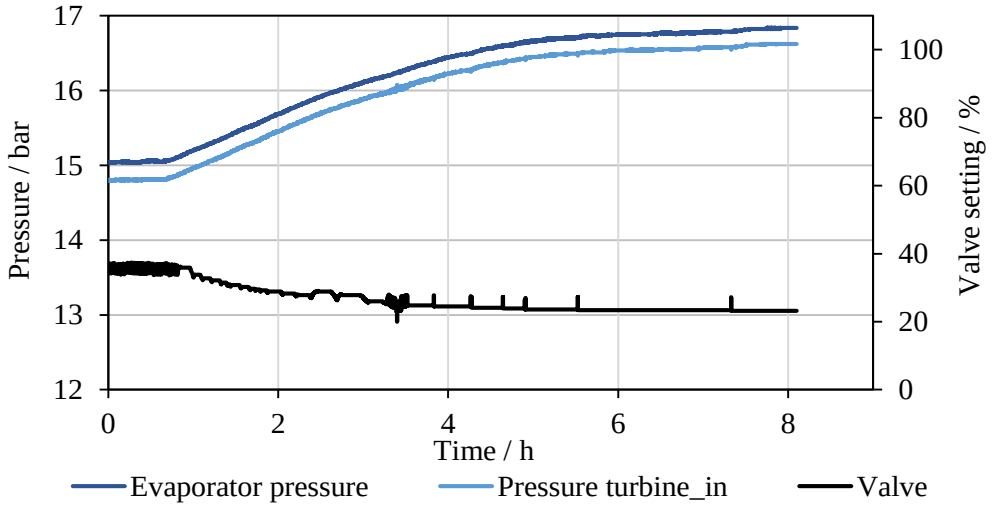

Figure 26. Storage process to 17 bar evaporator pressure, turbine inlet pressure and valve setting.

Figure 27 then shows, from a steady-state storage condition of approx. 17 bar, an abrupt opening of the valve within a few seconds, which causes the boiler pressure to drop and a sudden increase in turbine output from about 29 to over 33 kW_{el} over several minutes until the storage pressure returns to a steady state. It is also clearly evident that during throttled steady-state operation, there are additional losses due to the valve and the smaller pinch point in the evaporator, resulting in a slightly lower turbine output of approx. 1.0 kW_{el}.

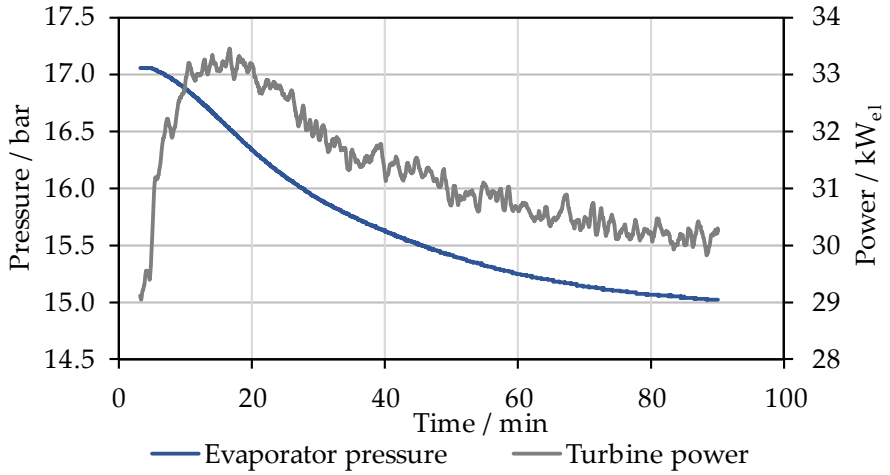

Figure 27. Turbine power during a sudden pressure release from 17 bar start condition.

Such an accumulation of steam can also be used to compensate for heating breakdowns. Figure 28a shows the pressure in the steam boiler and in the turbine inlet at a reduction in heating by 50% over approx. 9 min without control of the valve. The exhaust gas power and the resulting reduced turbine power can be seen in the right diagram.

In contrast, in Figure 29, a storage condition of 17 bar is considered, and during the reduction in exhaust power, the pressure upstream of the turbine is controlled to remain constant, also keeping the turbine power constant over this range. This method of storing steam could be predictively controlled, e.g., with a melting-free production plan in a die-casting process.

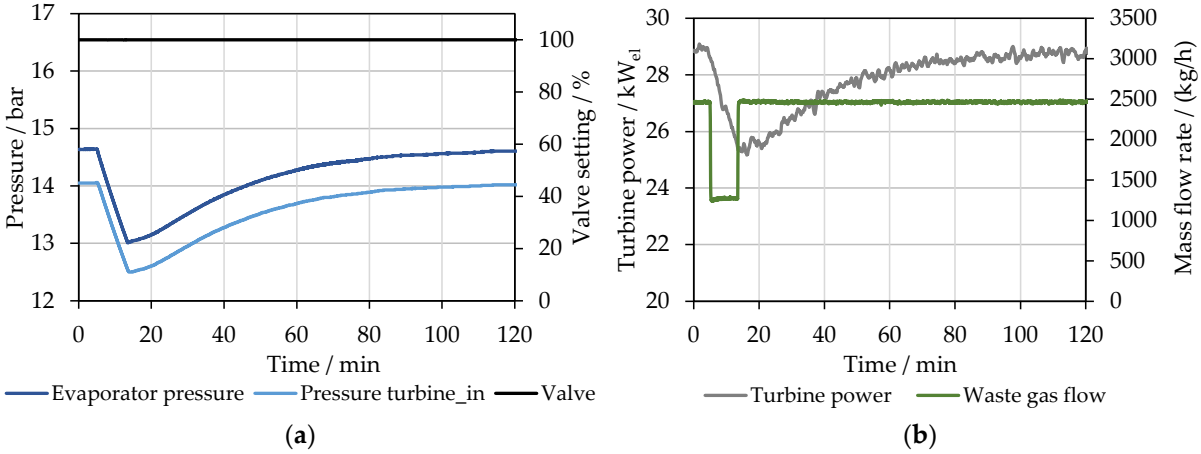

Figure 28. Evaporator pressure, inlet turbine pressure and valve setting (**a**); resulting turbine power and 50% drop in exhaust gas power (**b**) without previous storage.

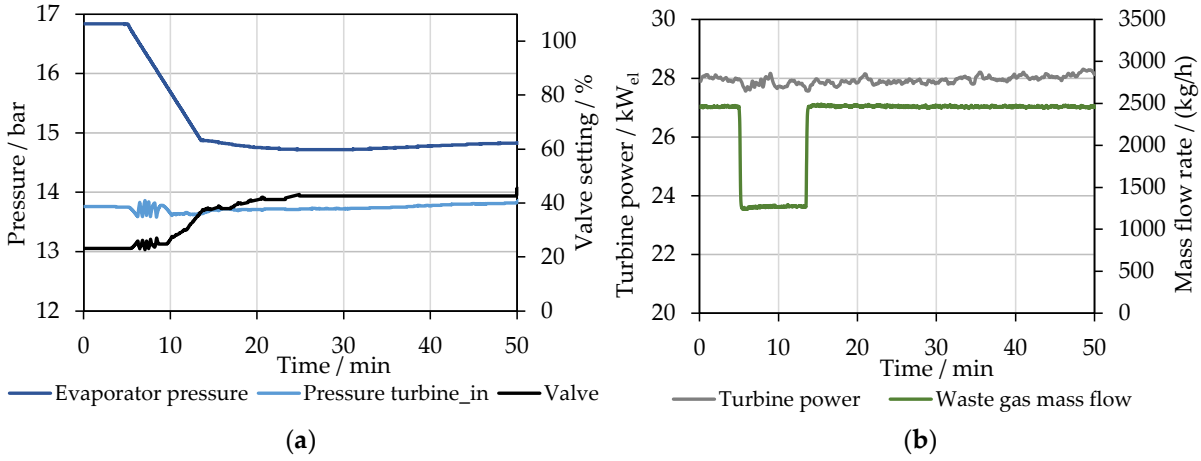

Figure 29. Evaporator pressure, inlet turbine pressure and controlled valve setting (**a**); resulting turbine power and 50% drop in exhaust gas power (**b**) with possible predictive storage.

In an SRC, a power peak can also be generated via a heat sink by storing cold. A sudden reduction in the cooling water temperature on the secondary side of the condenser leads to a reduction in the condensation pressure and thus an increase in the turbine power. The remaining heat in the exhaust gas, which leaves the evaporator at 170 °C in the design case, can serve as an energy source for generating cooling. If the maximum acceptable pressure drop in the exhaust system is not exceeded, additional deheating from 170 °C to 50 °C would correspond to an additional 165.0 kW_{th} in case of the MicroRankine plant, taking into account condensing technology [33]. Eligible absorption chillers with a Coefficient of Performance of 0.7 [34] would thus provide 115.6 kW of cooling capacity at 6 °C. A macro-encapsulated PCM in a water container was assumed as cold storage; it would occupy a total volume of 3.75 m^3 to store 125 kWh of cooling capacity [35] and would be able to discharge this into the cooling circuit of the SRC if required. This approach was tested in the MicroRankine setup, in which the river water mass flow rate was abruptly increased to reduce the inlet temperature of the intermediate circuit of the condenser by approx. 10 K. The mass flow rate in the intermediate circuit was kept constant. Figure 30 shows the condenser inlet temperature and turbine power during this test from minute five. Within about 20 min, the turbine power increased by about 2.5 kW_{el}. The assumed cold storage would be able to provide this additional cooling power over 56.7 min.

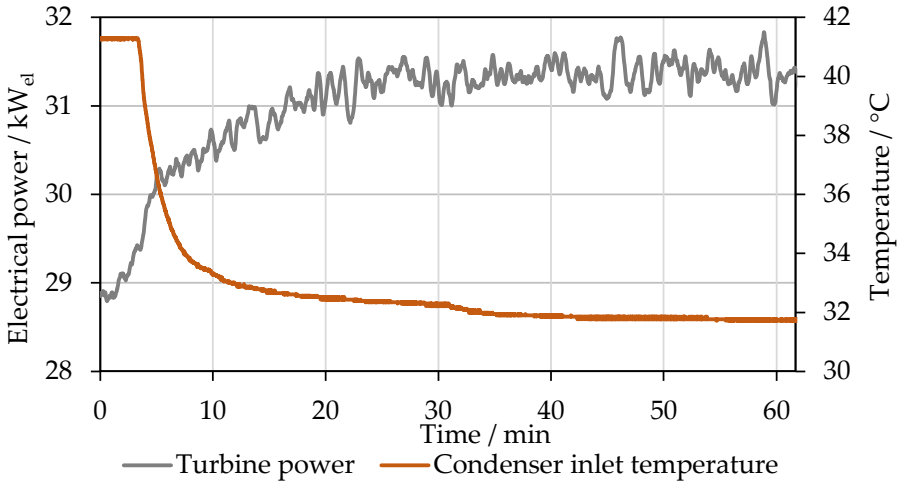

Figure 30. Turbine power during a sudden reduction in the heat sink inlet temperature.

3.3.2. Model-Based Investigation of Grid-Assistive Operation of Steam Storage Rankine Cycles

The storage capability of the system under investigation was expanded with the help of the fitted system model in order to be able to generate higher and longer power peaks. In addition to the storage pressure of approx. 17 bar (+2 bar) in the existing steam boiler with a storage volume of 1.27 m^3, the storage was expanded by 2000 L at the same pressure. In addition, a storage pressure of 30 bar (+15 bar) was simulated, and a combination of the increased storage volume and storage pressure was investigated. Figure 31 shows the steam boiler pressure and turbine output from steady-state storage conditions to a power peak and back to a steady state.

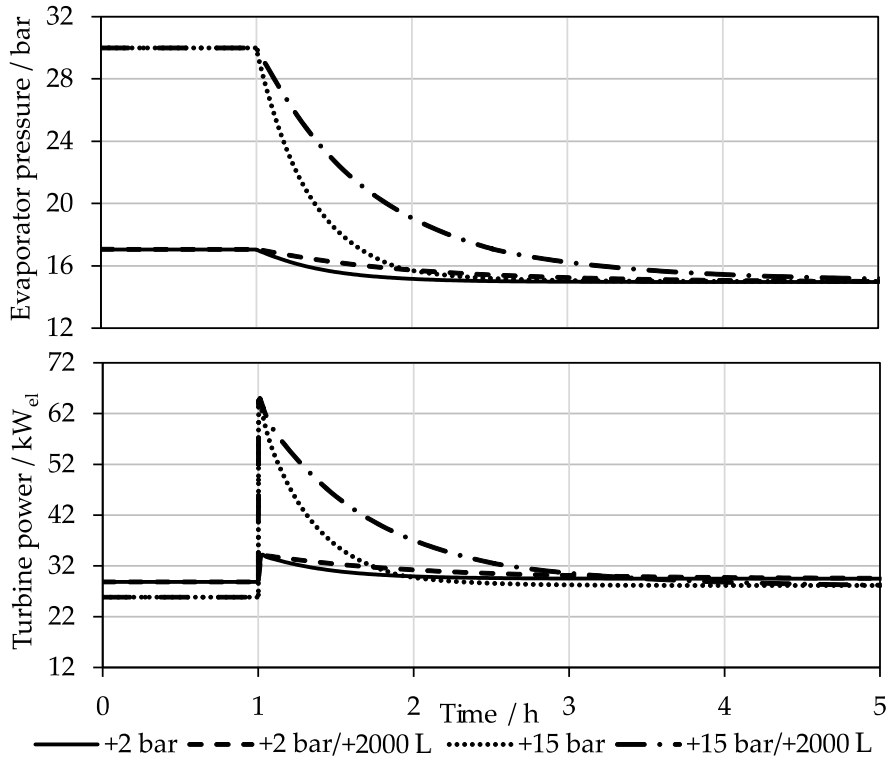

Figure 31. Simulated evaporator pressure and turbine power during power peak due to increased storage capacity of the steam boiler at +2 bar, +2000 L, +15 bar and +15 bar/2000 L.

Table 2 shows the maximum electrical power peak and the total electrical energy stored out for these cases compared to the steady state.

Table 2. Simulated maximum power peak and stored electrical energy with variations in the storage conditions.

		+2 bar	+2 bar/+2000 L	+15 bar	+15 bar/+2000 L
Power peak	[kW_{el}]	5.22	5.35	38.52	39.13
El. energy stored	[kWh_{el}]	3.28	5.39	16.37	28.62

Such stored-out power peak can contribute to peak shaving. For example, if an industrial company in Germany with an annual consumption of 300 MWh and a registered peak load of 120 kW can compensate the peak load of 38.52 kW_{el} shown in Figure 31 via the Steam Storage Rankine Cycle plant, this corresponds to an exemplarily additional annual saving of EUR 6,196 (depending on the location) [36]. With general electricity avoidance costs of 0.0896 EUR/kWh (the average industrial electricity price in Germany between 2012 and 2022 [37]) and an average output of 30 kW_{el} in 7500 operating hours, this corresponds to 30.7% more profit per year. The valve control discussed here can also be used for a load following operation such that the valve upstream of the turbine is adjusted to the actual load, thus delaying withdrawal.

In addition to the steam boiler, which must be designed for higher volumes or pressures, tubes, valves and other apparatuses must be adapted. A turbine that can handle such rapid load changes can be realized either in one machine via nozzle control or with a parallel turbine. The condenser and cooling system must be adequately sized for higher mass flow rates, or their thermal idleness must prevent exhaust pressures that are too high. The cold storage discussed in this section could cause additional turbine power during power peaks, especially in air-cooled plants, by keeping the exhaust steam pressure at a minimum. The pump in the system must also be able to cause a higher flow rate for a short time.

For the utilization of the storage capacity of an SRC plant with additional use for Power-2-Heat-Power on the grid operator's side, plants in larger power ranges seem to be particularly relevant. Short-term power peaks at grid nodes in the distribution grid, caused by renewable energies such as photovoltaics or fast charging stations, occur in the range of several hundred kW_{el}. These plant sizes could be provided in the transmission grid through pooling for FCR so that the minimum output of 1 MW_{el} is achieved, but plants with 1 MW_{el} of additional flexibility to receive or deliver power peaks are also conceivable. The technical feasibility of these capacities is provided by comparable plants; the storage concept in the steam boiler itself will reach its limits at some point. Parallel developments to steam storage could be used for this purpose [38,39].

If the last and largest power peak displayed in Figure 31 (+15 bar/+ 2000 L) would be realized by Power-2-Heat, the released 28.62 kWh_{el} would correspond to a storage efficiency of 13.3%. A parallel use of the surplus heat for feeding heat networks would significantly increase the overall efficiency. Despite these comparatively low efficiencies, Steam Storage Rankine Cycles can have an economic advantage over conventional systems through the parallel use of steady-state WHR and additional peak load shaving. Comparable electrochemical battery systems, or Carnot batteries, must generate their economic profitability exclusively through stored and unstored power peaks, which is why widespread use has not yet been achieved.

4. Conclusions

The appropriate use of different types of waste heat sources will be crucial, both as bridging technologies and in a CO_2-neutral future. An approach to the exergetic evaluation of waste heat is proposed in which not only the waste heat temperature but also possible further levels of a waste heat cascade are considered. Together with a techno-economic

evaluation, reasonable and sustainable decisions regarding different types of Waste Heat Recovery can be made.

This paper discusses the exploration of new applications for high-temperature WHR with a Steam Rankine Cycle, using the storage capability of the steam boiler. The Micro-Rankine SRC pilot plant at the Technische Hochschule Nürnberg served as the experimental platform. Here, 248 kW_{th} of exhaust gas power from a sewage gas engine at 450 °C is converted into electrical energy. The steam boiler has a liquid water content of 1.27 m^3 in a saturated state at various storage pressures. A dynamic system model was developed in Dymola/Modelica based on the physical transfer processes, fitted with steady-state and transient measurement data.

Subsequently, three specific applications were investigated with the help of experiments, and extensions were examined using the system model. First, the system's application as an Uninterruptible Power Supply was tested with the MicroRankine setup with different storage conditions and an abrupt switch-off of waste heat. The storage capacity of the steam boiler and the resulting turbine output were then modeled with higher storage pressures and storage volumes. The time in which electricity can be supplied to the grid can thus be doubled.

As a second application, the conversion of volatile waste heat and the smoothing of turbine output with the aid of storage and control over the valve upstream of the turbine were investigated. Using the system model, static and dynamic PI controllers with gain scheduling were first designed and then tested in the MicroRankine plant. Subsequently, the model itself was used to control the valve in a Model-Based Control. In each of the different experiments, an increase in control quality was achieved with increased control complexity. Afterwards, the system model was used to correct a step in the exhaust gas in a Model Predictive Control approach. The time back to the steady state was significantly reduced as a result. Additionally, with the help of the system model, the conversion of the real volatile waste heat profile of two crucible furnaces was investigated. In this case, the pressure upstream of the turbine could be kept constant with the already-existing storage dimensions. If systems such as the one presented are faced with similar control tasks, the possibility of implementation must first be examined, taking into account all boundary conditions. Depending on the application and the value of the desired control quality, a decision can ultimately be made in favor of one of the various approaches based on an economic analysis.

Finally, the use of the storage capability for grid-assistive operation was investigated. For this purpose, ways of creating power peaks in the MicroRankine plant were investigated experimentally. Afterwards, the integration of Power-2-Heat was presented, and through a model-based scale-up of the storage pressure and the storage volume in the steam boiler, short-term power peaks of more than 100% can be achieved.

Overall, it can be stated that there is potential for new applications regarding WHR with the Steam Storage Rankine Cycle. Further research is required before the system can be used in continuous operation in the investigated industrial environments in different power ranges. In addition to the experimental implementation of Power-2-Heat in the MicroRankine pilot plant, the increased storage capability of the steam boiler must be investigated and tested in future plants. In addition to the auxiliary equipment and apparatuses, the design of the boiler for frequent load changes must be taken into account.

Author Contributions: Conceptualization, F.R., L.B., F.O. and H.K., methodology, F.R., L.B., F.O. and H.K., experiments, F.R., simulation, F.R. and L.B., validation, F.R., formal analysis, F.R., L.B., F.O. and H.K., investigation, F.R. and F.O., resources, F.O., data curation, F.R., writing—original draft preparation, F.R., writing—review and editing, F.R., L.B., F.O. and H.K., visualization, F.R., supervision, F.O. and H.K., project administration, F.O., funding acquisition, F.O. All authors have read and agreed to the published version of the manuscript.

Funding: The MicroRankine pilot plant was funded by the German Federal Ministry of Education and Research as part of the FH-Invest 2016 program (13FH017IN6); the Bavarian State Ministry of Science and Arts kindly supported the project from its very beginning. Plant operation and experimental studies were carried out as part of the KompACT project, funded by the German Federal Ministry for Economics and Climate Action (03EE5010A). The authors highly appreciate these funds. This publication was funded by the Open Access Publishing Fund of the Technische Hochschule Nürnberg Gerog Simon Ohm.

Data Availability Statement: Data are contained within the article.

Acknowledgments: Within the entire test phase, the waste heat and space were provided by the Stadtentwässerung und Umweltanalytik Nürnberg, which the authors gratefully acknowledge.

Conflicts of Interest: The authors declare no conflicts of interest.

Nomenclature

Subscripts	
th	thermal
el	electrical
Abbreviations	
FCR	Frequency Containment Reserve
MBC	Model-Based Control
MPC	Model Predictive Control
ORC	Organic Rankine Cycle
PCM	Phase Change Material
PLC	Programmable Logic Controller
SRC	Steam Rankine Cycle
UPS	Uninterruptible Power Supply
WHR	Waste Heat Recovery

References

1. Forman, C.; Muritala, I.K.; Pardemann, R.; Meyer, B. Estimating the global waste heat potential. *Renew. Sustain. Energy Rev.* **2015**, *57*, 1568–1579. [CrossRef]
2. German Federal Office of Statistics. Number of Operational Coal Power Plants Worldwide as of July 2022, by Country/Territory. 2022. Available online: https://www.statista.com/statistics/859266/number-of-coal-power-plants-by-country/ (accessed on 12 July 2023).
3. German Federal Office of Statistics. Distribution of Electricity Generation Worldwide in 2022, by Energy Source. 2022. Available online: https://www.statista.com/statistics/269811/world-electricity-production-by-energy-source/ (accessed on 12 July 2023).
4. Kalverkamp, M.; Pehlken, A.; Wuest, T. Cascade Use and the Management of Product Lifecycles. *Sustainability* **2017**, *9*, 1540. [CrossRef]
5. Kühn, A. *Abwärme—Rahmenbedingungen, Technische Potentiale und Betriebliche Risiken, Abwärme—Ein Unerschlossenes Potenzial der Wärmewende?* dena—Deutsche Energie-Agentur, Workshop: Henningsdorf, Germany, 2020.
6. Dehli, M. *Energieeffizienz in Industrie, Dienstleistung und Gewerbe*, 1st ed.; Springer Vieweg: Heidelberg, Germany, 2020; pp. 148–153.
7. Macchi, E.; Astolfi, M. *Organic Rankine Cycle (ORC) Power Systems*, 1st ed.; Woodhead Publishing: Cambridge, UK, 2017; p. 3.
8. Raab, F.; Klein, H.; Opferkuch, F. A Steam Rankine Cycle Pilot Plant for Distributed Waste Heat Recovery. In Proceedings of the 9th Heat Powered Cycles Conference, Bilbao, Spain, 10–13 April 2022.
9. Raab, F.; Klein, H.; Opferkuch, F. Steam Rankine Cycle instead of Organic Rankine Cycle for Distributed Waste Heat Recovery—Pros And Cons. In Proceedings of the 6th International Seminar on ORC Power Systems, Munich, Germany, 11–13 October 2021.
10. Baehr, H.D.; Kabalec, S. *Thermodynamik*, 16th ed.; Springer: Berlin/Heidelberg, Germany, 2016; pp. 166–170.
11. Ebeling, P. Konzeption eines Rankine-Prozesses für den Transienten Betrieb im Omnibus. Ph.D. Dissertation, Technischen Universität Braunschweig, Braunschweig, Germany, 2018.
12. Arreola, M.J.; Pili, R.; Magro, F.D.; Wieland, C.; Rajoo, S.; Romagnoli, A. Thermal power fluctuations in waste heat to power systems: An overview on the challenges and current solutions. *Appl. Therm. Eng.* **2018**, *134*, 576–584. [CrossRef]
13. Popp, T.; Weiß, A.P.; Heberle, F.; Winkler, J.; Scharf, R.; Weith, T.; Brüggemann, D. Experimental Characterization of an Adaptive Supersonic Micro Turbine for Waste Heat Recovery Applications. *Energies* **2020**, *15*, 25. [CrossRef]
14. Pili, R.; Romagnoli, A.; Spliethoff, H.; Wieland, C. Techno-Economic Analysis of Waste Heat Recovery with ORC from Fluctuating Industrial Sources. *Energy Procedia* **2017**, *129*, 503–510. [CrossRef]

15. Bause, T.; Campana, F.; Filippini, L.; Foresti, A.; Monti, N.; Pelz, T. Cogeneration with ORC at Elbe-Stahlwerke Feralpi EAF Shop. In Proceedings of the Iron & Steel Technology Conference and Exposition, Indianapolis, IN, USA, 5–8 May 2014.
16. Arabkoohsar, A. Combined steam based high-temperature heat and power storage with an Organic Rankine Cycle, an efficient mechanical electricity storage technology. *J. Clean. Prod.* **2020**, *247*, 119098. [CrossRef]
17. Nardin, G.; Meneghetti, A.; Magro, F.D.; Benedetti, N. PCM-based energy recovery from electric arc furnaces. *Appl. Energy* **2014**, *136*, 947–955. [CrossRef]
18. Pantaleo, A.M.; Fordham, J.; Oyewunmi, O.; De Palma, P.; Markides, C.N. Integrating cogeneration and intermittent waste-heat recovery in food processing: Microturbines vs. ORC systems in the coffee roasting industry. *Appl. Energy* **2018**, *225*, 782–796. [CrossRef]
19. Murakoshi, R.; Fushimi, C. Integration of a steam accumulator with a biomass power-generation system for flexible energy storage and discharge: Effect of the initial steam pressure on the steam discharge profile and levelized cost of storage. *J. Energy Storage* **2022**, *55*, 105586. [CrossRef]
20. Schlüter, W.; Hanna, J.; Zacharias, K. Simulationsbasierte Dimensionierung von Regeneratoren für eine volatile Hochtemperatur-Abwärmeverstromung. In Proceedings of the ASIM SST 2020, 25. Symposium Simulationstechnik, Virtual, 14–15 October 2020; pp. 281–288.
21. *DIRECTIVE 2014/68/EU of the European Parliament and of the Council of 15 Mai 2014 on the Harmonisation of the Laws of the Member States Relating to the Making Available on the Market of Pressure Equipment*; Beuth Verlag GmbH: Berlin, Germany, 2014.
22. Goldstern, W. *Dampfspeicheranlagen. Elemente, Prinzip, Aufbau und Berechnung der Gefälle- und Gleichdruckspeicher Sowie Anwendung und Wirtschaftlichkeit*, 1st ed.; Springer: Berlin/Heidelberg, Germany, 1933.
23. Hofmann, R.; Dusek, S.; Gruber, S.; Drexler-Schmid, G. Design Optimization of a Hybrid Steam-PCM Thermal Energy Storage for Industrial Applications. *Energies* **2019**, *12*, 898. [CrossRef]
24. Schulze, C. A Contribution to Numerically Efficient Modelling of Thermodynamic Systems. Ph.D. Dissertation, Technischen Universität Braunschweig, Braunschweig, Germany, 2013.
25. *DIN 60534-2-1*; Industrial-Process Control Valves—Part 2-1: Flow Capacity—Sizing Equations for Fluid Flow under Installed Conditions (IEC 60534-2-1:2011); German version EN 60534-2-1:2011. Beuth Verlag GmbH: Berlin, Germany, 2012.
26. *DIN 60534-2-3*; Industrial-Process Control Valves—Part 2-3: Flow Capacity—Test Procedures (IEC 60534-2-3:2015); German version EN 60534-2-3:2016. Beuth Verlag GmbH: Berlin, Germany, 2017.
27. *DIN EN IEC 62040-3*VDE 0558-530*; Uninterruptible Power Systems (UPS)—Part 3: Method of Specifying the Performance and Test Requirements (IEC 62040-3:2021); German version EN IEC 62040-3:2021. Beuth Verlag GmbH: Berlin, Germany, 2022.
28. Stephan, W.; Zitzmann, K.; Pröbstle, G.; Kapischke, J. *Effiziente Energieversorgung in der Industrie—Teilprojekt "Metallschmelzbetriebe" Effiziente Energienutzung in Nicht-Eisen-Metall-Schmelzbetrieben, Effiziente Energienutzung in Nicht-Eisen-Metall-Schmelzbetrieben, Bayer*; Landesamt für Umweltschutz: Augsburg, Germany, 2005.
29. Zapf, M.; Blenk, T.; Müller, A.C.; Pengg, H.; Mladenovic, I.; Weindl, C. Lifetime Assessment of PILC Cables with Regard to Thermal Aging Based on a Medium Voltage Distribution Network Benchmark and Representative Load Scenarios in the Course of the Expansion of Distributed Energy Resources. *Energies* **2021**, *14*, 494. [CrossRef]
30. Bundesnetzagentur für Elektrizität, Gas, Telekommunikation, Post und Eisenbahnen. Redispatch. Available online: https://www.bundesnetzagentur.de/DE/Fachthemen/ElektrizitaetundGas/Versorgungssicherheit/Netzengpassmanagement/Engpassmanagement/Redispatch/start.html (accessed on 12 July 2023).
31. 50Hertz Transmission GmbH; Amprion GmbH; TenneT TSO GmbH; TransnetBW GmbH. Plattform für Regelenergie. Available online: https://www.regelleistung.net/de-de/ (accessed on 12 July 2023).
32. German Federal Ministry of Justice. Stromnetzzugangsverordnung from July 25th 2005 (BGBl. I S. 2243), Last Revised by Article 6 of the Act of July 2021 (BGBl. I p. 3026). Available online: https://www.gesetze-im-internet.de/stromnzv/BJNR224300005.html (accessed on 12 July 2023).
33. Gundermann, M.; Raab, F.; Raab, D.; Botsch, T.W. Investigation of the heat transfer coefficient during the condensation of small quantities of water vapour from a mixture with a high proportion of non-condensable gas in a horizontal smooth tube. *Int. J. Heat Mass Transf.* **2021**, *170*, 121016. [CrossRef]
34. Stürzebecher, W.; Heyse, C. Blockheizkraftwerke und Absorptionskältemaschinen. Hocheffiziente Strom-Wärme-Kälte-Erzeugung in Gewerbe und Industrie. *Kälte Klima Aktuell* **2020**, *1/2020*. Available online: https://www.kka-online.info/artikel/kka_Blockheizkraftwerke_und_Absorptionskaeltemaschinen-3497789.html (accessed on 12 July 2023).
35. Jona, S.; Klara Energy Systems GmbH. HeatStixx. Personal communication, 2022.
36. Strom- und Gasnetz Wismar GmbH. Erläuterungen zu den Netznutzungsentgelten. Available online: https://www.sg-wismar.de/fileadmin/user_upload/ID064_Netznutzung_Strom/ID354_Netznutzungsentgelte/221228_Erl.Preisblatt_2023_per_31.12.pdf (accessed on 12 July 2023).
37. German Federal Office of Statistics. Industriestrompreise in Deutschland in den Jahren 2001 bis 2022. 2022. Available online: https://de.statista.com/statistik/daten/studie/155964/umfrage/entwicklung-der-industriestrompreise-in-deutschland-seit-1995/ (accessed on 8 January 2024).

38. Schäfer, T. Thermo-Mechanischer Stromspeicher (CARNOT-Batterie), invited Presentation, CLEANTECH Initiative Ostdeutschland Arbeitskreis Energiespeicher, 11.06.2020.
39. Stevanovic, V.D.; Petrovic, M.M.; Milivojevic, S.; Ilic, M. Upgrade of the thermal power plant flexibility by the steam accumulator. *Energy Convers. Manag.* **2020**, *223*, 113271. [CrossRef]